AIP | Applied Physics Letters

Electron tunneling through atomically flat and ultrathin hexagonal boron nitride

Gwan-Hyoung Lee, Young-Jun Yu, Changgu Lee, Cory Dean, Kenneth L. Shepard et al.

Citation: Appl. Phys. Lett. **99**, 243114 (2011); doi: 10.1063/1.3662043
View online: http://dx.doi.org/10.1063/1.3662043
View Table of Contents: http://apl.aip.org/resource/1/APPLAB/v99/i24
Published by the American Institute of Physics.

Electron tunneling through atomically flat and ultrathin hexagonal boron nitride

Gwan-Hyoung Lee,[1,2] Young-Jun Yu,[3] Changgu Lee,[4] Cory Dean,[1,5] Kenneth L. Shepard,[5] Philip Kim,[3] and James Hone[1,a)]
[1]*Department of Mechanical Engineering, Columbia University, New York, New York 10027, USA*
[2]*Samsung-SKKU Graphene Center (SSGC), Suwon 440-746, Korea*
[3]*Department of Physics, Columbia University, New York, New York 10027, USA*
[4]*Department of Mechanical Engineering, Sungkyunkwan University, Suwon 440-746, Korea*
[5]*Department of Electrical Engineering, Columbia University, New York, New York 10027, USA*

(Received 11 October 2011; accepted 21 October 2011; published online 16 December 2011)

Electron tunneling through atomically flat and ultrathin hexagonal boron nitride (h-BN) on gold-coated mica was investigated using conductive atomic force microscopy. Low-bias direct tunneling was observed in mono-, bi-, and tri-layer h-BN. For all thicknesses, Fowler-Nordheim tunneling (FNT) occurred at high bias, showing an increase of breakdown voltage with thickness. Based on the FNT model, the barrier height for tunneling (3.07 eV) and dielectric strength (7.94 MV/cm) of h-BN are obtained; these values are comparable to those of SiO_2. © *2011 American Institute of Physics*. [doi:10.1063/1.3662043]

The excellent properties of graphene have stimulated interest in two-dimensional crystals of other conducting and semiconducting materials.[1–3] These materials require ultraflat and low-disorder dielectric layers for device fabrication. However, charged impurities in traditional oxides or high-k dielectrics introduce disorder that can degrade mobility and performance of ultrathin field effect transistors (FET).[4] Moreover, gate oxides with thickness less than 5 nm have been studied for metal-oxide-semiconductor field effect transistors (MOSFETs). For such ultrathin gate oxides, control of the thickness and uniformity is particularly important for reliability and long term stability of MOSFETs.[5,6]

Recently, hexagonal boron nitride (h-BN), which is an isomorph of graphene and an insulator with a wide band gap (5.2–5.9 eV),[7–9] was employed as an improved dielectric for graphene devices.[10] Since h-BN is chemically and thermally stable and free of dangling bonds and surface charge traps, graphene devices on h-BN show roughness and fluctuations in potential two orders of magnitude lower than comparable devices on SiO_2,[11,12] which in turn leads to improved mobility, FET performance, and chemical stability.[10,13,14]

Conductive atomic force microscopy (C-AFM) has been used for current measurements in various systems such as thin oxide layers,[5,6,15] self-assembled monolayers (SAMs),[16] single molecules,[17] and proteins.[18] C-AFM is a useful tool for current measurements of nanoscale materials and for studying spatial variability of electronic properties. In particular, mapping by C-AFM can be used to determine whether the breakdown voltage is uniform or shows local variation due to defects in the crystal structure. In this letter, we measure electron tunneling through atomically flat and ultrathin h-BN using C-AFM. The measurements reveal homogeneously insulating behavior and the absence of charged impurities and defects. The data can be used to calculate the barrier height and dielectric strength in a Fowler-Nordheim tunneling (FNT) model.

A thin (10 nm) layer of gold was first deposited on mica to create an atomically flat and conductive substrate. Next, h-BN powder (Momentive Performance Inc.) was mechanically exfoliated onto the gold-coated mica. C-AFM (XE-100, Park Systems) was utilized to measure current as shown in Fig. 1(a). A platinum wire tip (PtProm 10 M_T, Park Systems) of Fig. 1(b) was used to avoid loss of conductivity due to wear. h-BN thicker than three layers could be identified with optical microscopy, whereas the thinner h-BN was almost optically invisible on the gold-coated mica due to low optical contrast difference. Therefore, to create mono- and bi-layer h-BN samples, h-BN was first exfoliated on a Si wafer covered with 295 nm-thick SiO_2, on which substrate thin flakes could be located by optical microscopy. The flakes were then transferred to the gold-coated mica by spin-coating polymethyl methacrylate (PMMA), delaminating the PMMA in KOH, floating the membrane on water, and finally transferring it onto gold-coated mica with heating at 130 °C for drying of water and good adhesion. Finally, the PMMA was removed by dipping a sample in acetone for a day.

Figures 2(a) and 2(b) show optical and topographic AFM images of h-BN flakes on gold-coated mica. The surfaces are atomically flat (within the resolution of the AFM), as seen previously.[19] Figure 2(c) shows conductance AFM image of h-BN flakes with different thicknesses. This image demonstrates that the tunneling current is a function of

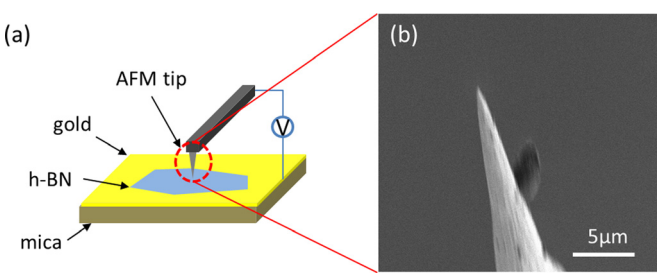

FIG. 1. (Color online) (a) Schematic picture of measurement set-up in C-AFM, (b) SEM image of platinum wire AFM tip.

a)Author to whom correspondence should be addressed. Electronic mail: jh2228@columbia.edu.

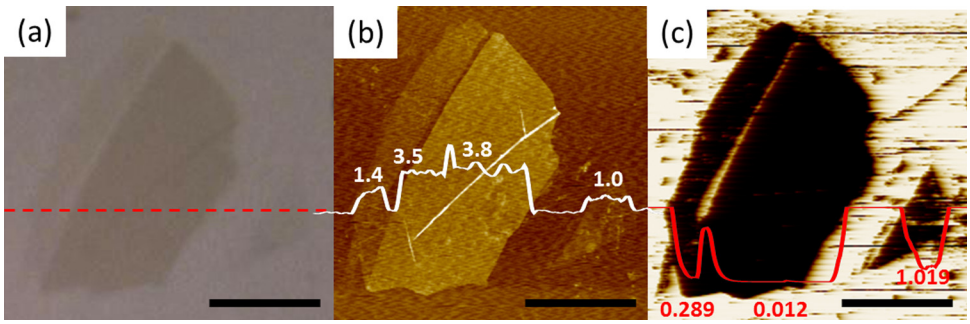

FIG. 2. (Color online) (a) Optical microscopic image, (b) topological, and (c) conductance AFM images of h-BN flakes on gold-coated mica. The profile lines of (b) and (c) show changes of thickness (nm) and current (nA) along dashed line of (a), respectively. The limit of current which can be measured in C-AFM is 10 nA. Conductance AFM image of (c) was acquired using a tip bias of 1 V. The scale bar is 5 μm.

thickness, as expected, and that the insulating quality is uniform within areas of the same thickness.

Figure 3(a) shows *I-V* curves taken for a 3 nm-thick h-BN flake at different loading forces. The curves show linear behavior at low bias due to direct tunneling and a sharp turn-on above ~3.5 V. Up to ~2nN, the low-bias current increases with force most probably due to the increase in the contact area between the tip and h-BN with increasing loading force,[18] after which the curves are virtually identical. Similarly, the low-bias tunnel conductance (dI/dV), as shown in the inset of Fig. 3(a) saturates over 2nN. Thin water layer might form between h-BN and the AFM tip. However, increase of current at higher sample-tip forces and stable *I-V* curves indicates that water layer does not play a role in this measurement. Therefore, for all subsequent experiments, a loading force of 2nN was used. Small asymmetry the measured current-voltage (I-V) curves has been attributed to the non-uniformity of electric field between the AFM tip and the gold-coated mica, which results in reduction of an attractive force between the tip and the sample and also the polarity dependent tunneling barrier shape.[18] However, this asymmetry behavior is small enough to be neglected.

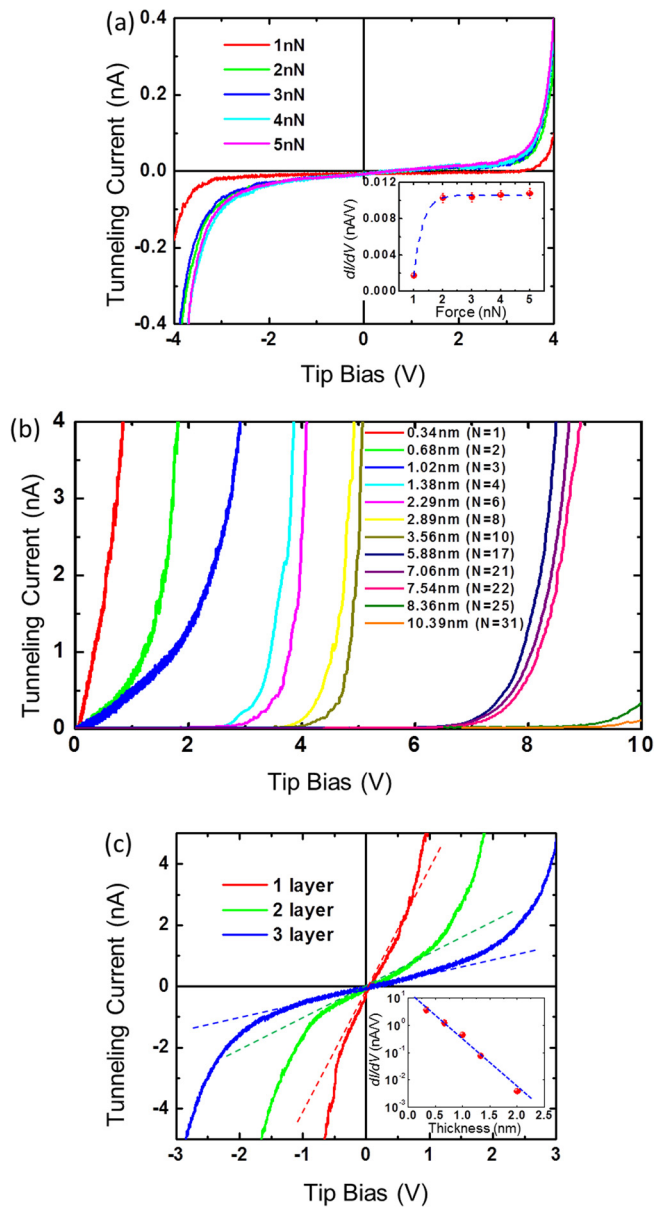

FIG. 3. (Color online) *I-V* measurements (a) in 3 nm-thick h-BN with various loading forces and (b) in h-BN of various thicknesses (N = layer number) with fixed loading force of 2nN. Inset of (a) shows tunnel conductance in the linear regime of small tip bias with different loading forces. (c) *I-V* curves of mono-, bi-, and tri-layer h-BN. Inset of (c) shows log-scale tunnel conductance in the linear regime (direct tunneling).

Figure 3(b) shows *I-V* measurements of h-BN flakes with various thicknesses from 1-31 layers. Mono-, bi-, and tri-layer samples show measurable low-bias conductance, which we ascribe to direct tunneling. Thicker samples are insulating at low bias and show sharp increases at a breakdown voltage that increases with thickness. The low-bias region is highlighted in Fig. 3(c). The inset shows the conductance as a function of sample thickness, which decays exponentially, as expected for direct tunneling.[20] At low bias voltage (V), where the tunneling barrier is not deformed severely by the applied electric field, the tunneling current (I) simply linearly depends on V as follows:[21]

$$I(V) = \frac{A_{eff}\sqrt{m\phi_B}q^2V}{h^2 d}\exp\left[\frac{-4\pi\sqrt{m\phi_B}d}{h}\right], \qquad (1)$$

where A_{eff} and ϕ_B are, respectively, effective contact area and barrier height. The values of q, m, d, and h are electron charge, free electron mass, separation between the two electrodes, and Plank's constant, respectively. Although Eq. (1) describes the observed exponential decay of tunneling current in d, further quantitative analysis is difficult since A_{eff} and ϕ_B are convoluted in the linear tunneling conductance.

In a high bias regime, the tunneling process is dominated by field-emission tunneling across the barrier and the tunneling current becomes non-linear. We analyze the high-bias data using the Fowler-Nordheim tunneling theory. The equation for FNT can be expressed as follows:[6,15,22–24]

$$I(V) = \frac{A_{eff}q^3mV^2}{8\pi h\phi_B d^2 m^*}\exp\left[\frac{-8\pi\sqrt{2m^*}\phi_B^{\frac{3}{2}}d}{3hqV}\right], \qquad (2)$$

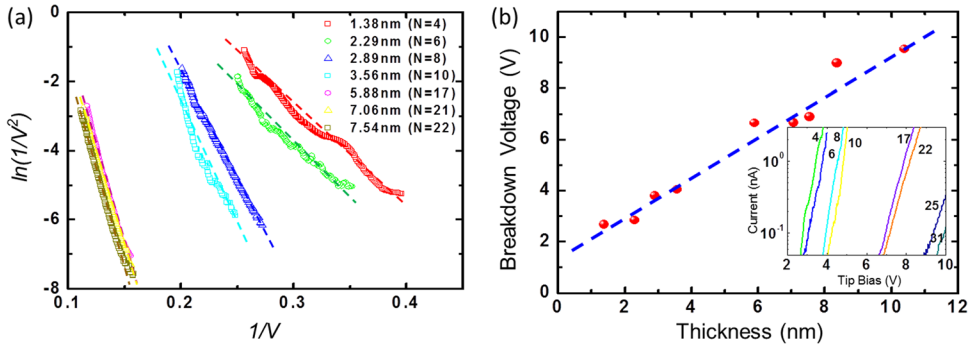

FIG. 4. (Color online) (a) *ln(I/V2)* vs. *1/V* curves for fitting of Fowler-Nordheim tunneling model. From linear fitting of curves, barrier height of 3.07 eV (±0.3) for tunneling was calculated. (b) Change of breakdown voltage with thickness of h-BN. The slope of linear fitting in (b) shows dielectric strength of ultrathin h-BN (7.94 MV/cm). Inset of (b) shows log-scale tunnel current curves to determine breakdown voltages for h-BN of various thicknesses, where numbers represent layer of h-BN.

where m^*/m is 0.26 for h-BN with the bare electron mass m.[25] This equation then can be reexpressed as

$$\ln\frac{I(V)}{V^2} = \ln\frac{A_{eff}q^3m}{8\pi h\phi_B d^2 m^*} - \frac{8\pi\sqrt{2m^*}\phi_B^{\frac{3}{2}}d}{3hqV}. \quad (3)$$

Figure 4 shows the measured tunneling current presented in $ln(I(V)/V^2)$ versus $1/V$ for each different thickness at the high bias regime. A strong linear dependence in this plot, which can be best fitted by Eq. (3), indicates that the tunneling through h-BN at high bias can be explained by FNT model. From the slope of each curve, the barrier height (ϕ_B) of 3.07 eV (±0.3) is obtained, which is comparable to that of SiO_2 (3.25 eV).[5] Variation in the calculated barrier height is attributed to the instrumental offset of AFM in h-BN thickness measurement,[26] absorbed water layer on h-BN,[15] and tip contamination.[23] From intercept of Eq. (3), we estimate that effective contact area (A_{eff}) in this measurement is 5.71×10^{-16} m^2 in average, corresponding to a circular contact area with diameter of 25 nm (±10 nm).

At the extreme high bias limit before failure of the device, tunneling current starts to increase exponentially, signaling the dielectric breakdown of h-BN. The inset of Fig. 4(b) shows this exponential increase in I as a function of V in the breakdown regime for different thicknesses of h-BN. In this work, the dielectric break down voltage (V_{break}) was obtained using the constant current method (the voltage at which the current reaches 10^{-11}A).[27] From linear increase of V_{break} with increasing number of h-BN layers we estimate the dielectric breakdown strength of 7.94 MV/cm. We note that this value is close to that of SiO_2 (8-10 MV/cm),[28] suggesting that h-BN can replace SiO_2 with a similar insulating characteristics but with less charge impurities, better uniformity and atomically flat surface for applications requiring high quality controlled tunnel barriers.

In summary, electron tunneling characteristics of atomically flat and ultrathin h-BN was studied using C-AFM. From C-AFM images, uniform and excellent insulating properties of ultrathin h-BN are demonstrated. Direct tunneling was observed in thin h-BN of mono-, bi-, and tri-layer. At high bias regime, Fowler-Nordheim tunneling occurred in h-BN thicker than four layers. We estimate the barrier height for tunneling and dielectric breakdown strength of h-BN are 3.03 eV (±0.3) and 7.94 MV/cm, respectively. These results confirmed that h-BN is the most promising candidate for ultrathin insulator and gate dielectric.

This work was supported by the NSF under Grant No. DMR-1122594, FENA FCRP, Air Force MURI, and DARPA under the CERA program.

[1]K. S. Novoselov, A. K. Geim, S. V. Morozov, D. Jiang, Y. Zhang, S. V. Dubonos, I. V. Grigorieva, and A. A. Firsov, Science **306**, 666 (2004).
[2]B. Radisavljevic, A. Radenovic, J. Brivio, V. Giacometti, and A. Kis, Nat. Nanotechnol. **6**, 147 (2011).
[3]N. Staley, J. Wu, P. Eklund, Y. Liu, L. Li, and Z. Xu, Phys. Rev. B **80**, 184505 (2009).
[4]B. Fallahazad, S. Kim, L. Colombo, and E. Tutuc, Appl. Phys. Lett. **97**, 123105 (2010).
[5]M. Hirose, Mater. Sci. Eng., B **41**, 35 (1996).
[6]A. Olbrich, B. Ebersberger, and C. Boit, Appl. Phys. Lett. **73**, 3114 (1998).
[7]X. Blase, A. Rubio, S. G. Louie, and M. L. Cohen, Phys. Rev. B **51**, 6868 (1995).
[8]D. M. Hoffman, G. L. Doll, and P. C. Eklund, Phys. Rev. B **30**, 6051 (1984).
[9]K. Watanabe, T. Taniguchi, and H. Kanda, Nature Mater. **3**, 404 (2004).
[10]C. R. Dean, A. F. Young, I. Meric, C. Lee, L. Wang, S. Sorgenfrei, K. Watanabe, T. Taniguchi, P. Kim, K. L. Shepard, and J. Hone, Nat. Nanotechnol. **5**, 722 (2010).
[11]J. Xue, J. Sanchez-Yamagishi, D. Bulmash, P. Jacquod, A. Deshpande, K. Watanabe, T. Taniguchi, P. Jarillo-Herrero, and B. J. Leroy, Nature Mater. **10**, 282 (2011).
[12]R. Decker, Y. Wang, V. W. Brar, W. Regan, H. Z. Tsai, Q. Wu, W. Gannett, A. Zettl, and M. F. Crommie, Nano Lett. **11**, 2291 (2011).
[13]S. Mayorov, R. V. Gorbachev, S. V. Morozov, L. Britnell, R. Jalil, L. A. Ponomarenko, P. Blake, K. S. Novoselov, K. Watanabe, T. Taniguchi *et al.*, Nano Lett. **11**, 2396 (2011).
[14]W. Gannett, W. Regan, K. Watanabe, T. Taniguchi, M. F. Crommie, and A. Zettl, Appl. Phys. Lett. **98**, 242105 (2011).
[15]A. Ando, R. Hasunuma, T. Maeda, K. Sakamoto, K. Miki, Y. Nishioka, and T. Sakamoto, Appl. Surf. Sci. **162–163**, 401 (2000).
[16]Y. B. Qi, I. Ratera, J. Y. Park, P. D. Ashby, S. Y. Quek, J. B. Neaton, and M. Salmeron, Langmuir **24**, 2219 (2008).
[17]X. D. Cui, A. Primak, X. Zarate, J. Tomfohr, O. F. Sankey, A. L. Moore, T. A. Moore, D. Gust, G. Harris, and S. M. Lindsay, Science **294**, 571 (2001).
[18]D. Xu, G. D. Watt, J. N. Harb, and R. C. Davis, Nano Lett. **5**, 571 (2005).
[19]C. H. Lui, L. Liu, K. F. Mak, G. W. Flynn, and T. F. Heinz, Nature **462**, 339 (2009).
[20]L. A. Bumm, J. J. Arnold, T. D. Dunbar, D. L. Allara, and P. S. Weiss, J. Phys. Chem. B **103**, 8122 (1999).
[21]J. G. Simmons, J. Appl. Phys. **34**, 2581 (1963).
[22]R. H. Fowler and L. Nordheim, Proc. R. Soc. London, Ser. A **119**, 173 (1928).
[23]W. Frammelsberger, G. Benstetter, J. Kiely, and R. Stamp, Appl. Surf. Sci. **252**, 2375 (2006).
[24]Y. Miyamoto, A. Yamaguchi, K. Oshima, W. Saitoh, and M. Asada, J. Vac. Sci. Technol. B **16**, 851 (1998).
[25]Y. N. Xu and W. Y. Ching, Phys. Rev. B **44**, 7787 (1991).
[26]A. Gupta, G. Chen, P. Joshi, S. Tadigadapa, and P. C. Eklund, Nano Lett. **6**, 2667 (2006).
[27]K. Boucart and A. M. Ionescu, Solid State Electron. **52**, 1318 (2008).
[28]S. N. Mohammad, F. J. Kub, and C. R. Eddy, J. Vac. Sci. Technol. B **29**, 021021 (2011).